Journal of ELECTRONIC MATERIALS, Vol. 41, No. 6, 2012
DOI: 10.1007/s11664-011-1886-4

Effect of GaSb Addition on the Thermoelectric Properties of $Mg_2Si_{0.5}Sn_{0.5}$ Solid Solutions

Z.L. DU,[1] G.Y. JIANG,[1] Y. CHEN,[1] H.L. GAO,[1] T.J. ZHU,[1] and X.B. ZHAO[1,2]

1.—State Key Laboratory of Silicon Materials, Department of Materials Science and Engineering, Zhejiang University, Hangzhou 310027, People's Republic of China. 2.—e-mail: zhaoxb@zju.edu.cn

$Mg_2Si_{0.5}Sn_{0.5}$-xGaSb ($0 \le x \le 0.15$) solid solutions were synthesized by a B_2O_3 flux method followed by hot pressing. X-ray power diffraction analysis and scanning electron microscopy observations confirm that single-phase samples were obtained. The lattice constant monotonically increases with increasing GaSb content. It was found that the Seebeck coefficients showed weak temperature dependency after alloying with GaSb, being enhanced at high temperatures. The electrical conductivity increases while the lattice thermal conductivity decreases with increasing GaSb content. A maximum dimensionless figure of merit of 0.47 was obtained at 660 K for the sample with $x = 0.08$, mainly due to its high electrical conductivity.

Key words: Magnesium silicides, thermoelectric properties, thermoelectric materials, isoelectronic substitution

INTRODUCTION

Thermoelectric (TE) devices are all solid state, noiseless, and maintenance free and can directly convert heat from different sources such as solar heat, geothermal heat, and exhaust gases from automobiles into electricity.[1,2] Their conversion efficiency depends on the materials' dimensionless figure of merit $ZT = \alpha^2\sigma T/\kappa$, where α is the Seebeck coefficient, σ is the electrical conductivity, κ is the thermal conductivity, and T is the temperature in Kelvin. Although conventional Bi_2Te_3[3] and PbTe-based alloys[4] exhibit good TE performance, their constituent elements are toxic and rare on Earth. An ideal TE material should not only have high ZT but should also be nontoxic and abundant in nature. These issues make the $Mg_2(Si,Sn)$-based TE material system a good candidate for TE conversion.

High $ZT \ge 1$ has been obtained in $Mg_2(Si,Sn)$ solid solutions.[5,6] The light constituent elements result in relatively higher thermal conductivity of about 2 W m^{-1} K^{-1} to 4 W m^{-1} K^{-1},[5] compared with 1 W m^{-1} K^{-1} to 2 W m^{-1} K^{-1} for Bi_2Te_3,[7] 0.6 W m^{-1} K^{-1} to 1.3 W m^{-1} K^{-1} for $Ag_{2-y}Sb_yTe_{1+y}$ alloys,[8] and 0.7 W m^{-1} K^{-1} to 0.9 W m^{-1} K^{-1} for Zintl phase compounds.[9] This limits further improvements of ZT. We note that, in pure PbTe, isoelectronic substitution of Pb^{2+} by Ag^+ and Sb^{3+}, commonly known as LAST alloys, reduced the thermal conductivity and enhanced the TE performance due to the formation of AgSb-rich nanodots.[10] Yang et al.[11] also found that nanostructures serve as effective phonon scattering centers and enhance the TE performance of TAGS alloys, which can also be considered as partial isoelectronic substitution of Ge^{2+} in GeTe by Ag^+ and Sb^{3+}. This idea could be extended to $Mg_2(Si,Sn)$ solid solution by isoelectronic substitution of Si or Sn by both IIIA and VA atoms to lower the lattice thermal conductivity. For IIIA elements, boron and aluminum substitute the Mg site,[12,13] while gallium and indium substitute the Si site[12,14] in $Mg_2(Si,Sn)$ solid solutions. Therefore, gallium and indium are used for p-type substitution, and antimony for n-type substitution due to its large solubility limit of >37 mol% at the Si site in

(Received July 14, 2011; accepted December 21, 2011; published online January 28, 2012)

Mg_2Si.[15] However, our previous work indicated that the solubility of InSb (~5 mol%) is lower than that of GaSb (~15 mol%) in $Mg_2(Si,Sn)$ solid solutions. Therefore, in this work $Mg_2(Si,Sn)$ samples with different amounts of added GaSb ($0 \le x \le 0.15$) were synthesized and the effect of isoelectronic substitution of silicon or tin by gallium and antimony is investigated.

On the other hand, a facile B_2O_3 flux synthesis method has been successfully developed recently for preparation of Sb-doped $Mg_2Si_{1-x}Sn_x$ solid solutions, as conventional melting and ball milling synthesis methods[16,17] usually result in obvious oxidation and volatilization of magnesium during preparation of $Mg_2(Si,Sn)$ solid solutions. By using the newly developed B_2O_3 flux synthesis method, high ZT values of >0.9 have been reproducibly attained at $x = 0.5$.[18] Therefore, in this work the same B_2O_3 flux synthesis method is employed in the material preparation.

EXPERIMENTAL PROCEDURES

$Mg_2Si_{0.5}Sn_{0.5}$-xGaSb ($0 \le x \le 0.15$) compounds were synthesized by a B_2O_3 flux method in air.[18] Stoichiometric amounts of elemental Si (99.9%), Sn (99.5%), GaSb powders, and 10 mol% excess Mg (99%) powder were weighed, homogeneously mixed in an agate mortar, and then transferred into an alumina crucible. GaSb powder was prepared by melting Ga (99.99%) and Sb (99.9999%) granules at 1073 K for 10 h. After the starting materials were covered by B_2O_3 powders and compacted, the crucible was placed into a chamber furnace, heated at 973 K for 10 h, and finally cooled down to room temperature. After the alumina crucible was smashed, the B_2O_3 flux and the obtained product were easily separated from each other. The alloy ingots were ground and hot-pressed under pressure of 80 MPa at 1020 K for 2 h.

The phase structure was analyzed by x-ray diffraction (XRD) on a PANalytical X'Pert PRO diffractometer with Cu K_α radiation ($\lambda = 1.5406$ Å). The surfaces of the pellets were observed on a FEI Sirion® field-emission scanning electron microscope (FESEM). The thermal conductivity was calculated using $\kappa = D\rho C_p$, where ρ is the sample density estimated by an ordinary dimensional and weight measurement procedure, as shown in Table I. The thermal diffusivity D and specific heat C_p were measured by a laser flash method on a Netzsch LFA 457 apparatus with a Pyroceram standard. The errors in C_p and D are 7% and 3%, respectively, and the error in thermal conductivity is about 10%. The electrical conductivity and the Seebeck coefficient were measured on a computer-aided apparatus using a dc four-probe method and differential voltage/temperature technique, respectively. The errors in the measurement of electrical properties were evaluated to be within 5%.

RESULTS AND DISCUSSION

Figure 1a shows the XRD patterns of the hot-pressed $Mg_2Si_{0.5}Sn_{0.5}$-xGaSb samples (x = 0, 0.04, 0.06, 0.08, 0.10, 0.15). All the diffraction peaks can be indexed to the face-centered cubic (fcc) antifluorite structure with space group Fm-3m. The sample without GaSb addition has a weak Mg_2Sn-rich phase, which suggests that there exists a secondary phase of Mg_2Sn-rich solid solution for the composition $Mg_2Si_{0.5}Sn_{0.5}$ when using this method. However, no impurity phase was detected in the other samples, and the magnesium oxide peak is negligible, indicating that the B_2O_3 flux method is an effective way to prepare $Mg_2(Si,Sn)$ solid solutions. All diffraction peaks locate between those of pure Mg_2Si (JCPDS #35-0773) and Mg_2Sn (JCPDS #07-0274), indicating the formation of $Mg_2Si_{0.5}Sn_{0.5}$ solid solutions. The lattice parameters of $Mg_2Si_{0.5}Sn_{0.5}$-xGaSb samples are plotted in Fig. 1b, monotonically increasing from 6.572 Å to 6.587 Å with increasing GaSb content. Figure 1c shows a SEM image for the hot-pressed sample with $x = 0.08$. No remarkable impurity phases or compositional segregation were detected.

The temperature dependences of the electrical conductivity and Seebeck coefficient of the $Mg_2Si_{0.5}Sn_{0.5}$-xGaSb samples are shown in Fig. 2a and b. The electrical conductivity increases with temperature for all the samples, indicating semiconducting behavior. With increasing GaSb content the electrical conductivity first increases and then decreases. The electrical conductivity for $x = 0.08$ reaches 14.9×10^3 S m^{-1} at room temperature, about 110 times higher than that of $x = 0$ (0.13×10^3 S m^{-1}). Since isoelectronic substitution of GaSb should provide no electronic doping, the increased electrical conductivity probably comes from enhanced intrinsic carrier concentration

Table I. Some room-temperature properties of the $Mg_2Si_{0.5}Sn_{0.5}$-xGaSb samples

	$x = 0$	$x = 0.04$	$x = 0.06$	$x = 0.08$	$x = 0.10$	$x = 0.15$
ρ (g cm^{-3})	2.89	2.88	2.86	2.84	2.99	3.03
κ (W m^{-1} K^{-1})	2.1	2.1	2.0	2.0	1.9	1.7
σ (10^3 S m^{-1})	0.1	7.1	13.5	14.9	8.9	3.5
α (10^{-6} V K^{-1})	−285	−162	−165	−173	−200	−185

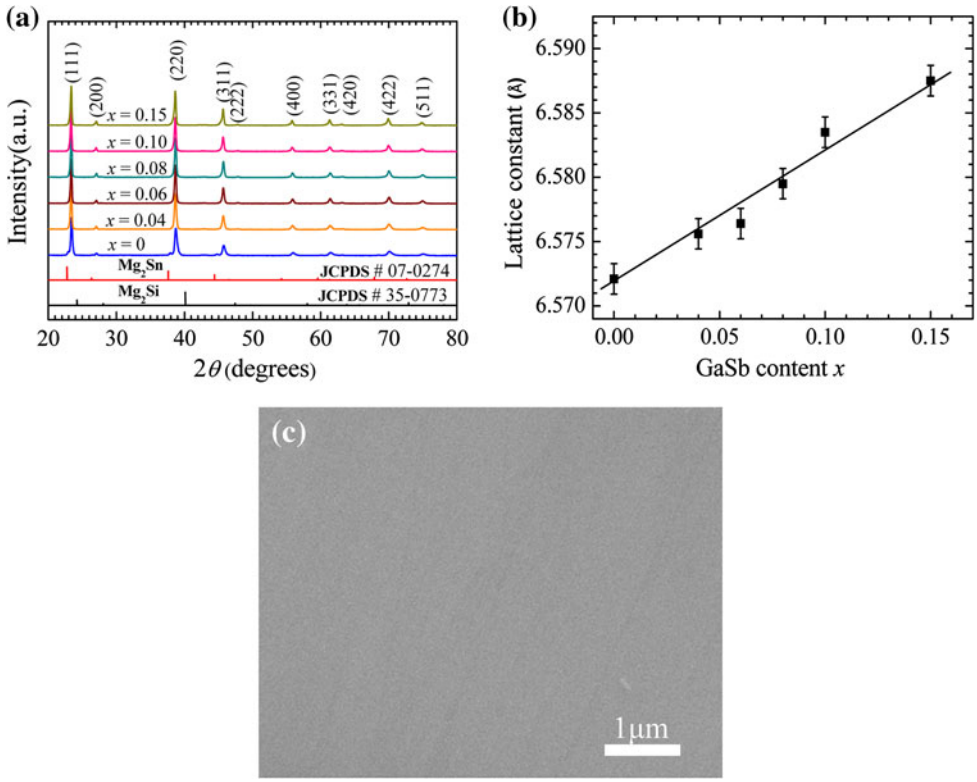

Fig. 1. (a) XRD patterns and (b) lattice constant of the $Mg_2Si_{0.5}Sn_{0.5}$-xGaSb ($0 \le x \le 0.15$) samples, and (c) SEM image for the sample with $x = 0.08$. The lattice constant increases monotonically from 6.572 Å to 6.587 Å with increasing GaSb content.

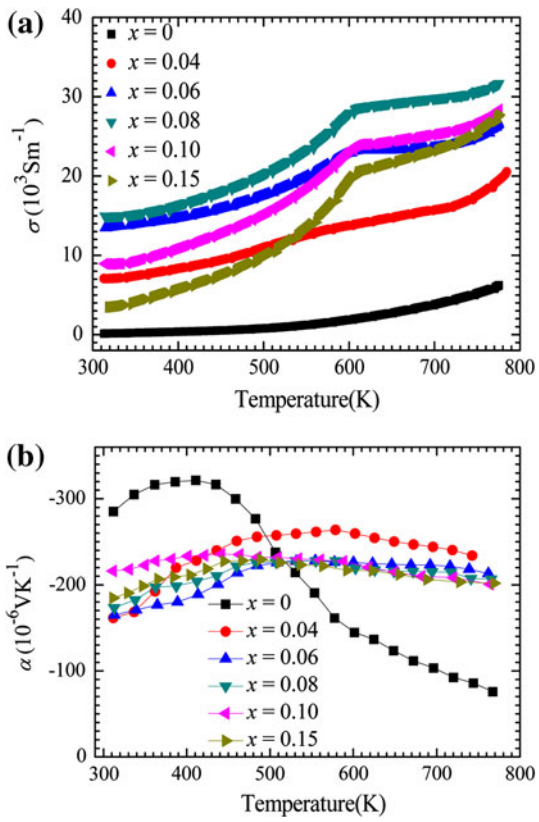

Fig. 2. Temperature dependences of (a) electrical conductivity σ and (b) Seebeck coefficient α for the $Mg_2Si_{0.5}Sn_{0.5}$-xGaSb samples.

contributed by interstitial Mg^{2+}[19] after addition of GaSb. For $x > 0.08$ the predominant ionic impurity scattering reduces the electron mobility and hence lowers the electrical conductivity. As a result, the $x = 0.08$ sample has the highest electrical conductivity over the temperature region of 300 K to 770 K. The electrical conductivity exhibits an unusual shoulder near 600 K, which coincides with the minimum in κ and maxima in α, suggesting a dominant bipolar conduction mechanism at high temperatures above 600 K.

The Seebeck coefficients are all negative in the measured temperature range with n-type conduction behavior, which possibly originates from the positively charged Mg ions at interstitial sites according to the calculation from Ref. 19. The Seebeck coefficient of the matrix increases to the maximum value at about 400 K and then drops with temperature dramatically due to intrinsic excitation, while the Seebeck coefficient of samples with added GaSb shows a slight decrease after bipolar conduction; for example, the Seebeck coefficient of the $x = 0.06$ sample only drops from -228 μV K^{-1} at 550 K to -213 μV K^{-1} at 760 K.

The thermal conductivity as a function of temperature for all the samples is shown in Fig. 3a. It first decreases and then increases with temperature due to intrinsic conduction. In the simplest case, the lattice thermal conductivity can be calculated by $\kappa = \kappa_l + L_0\sigma T$, where the Lorenz number $L_0 = 2 \times$

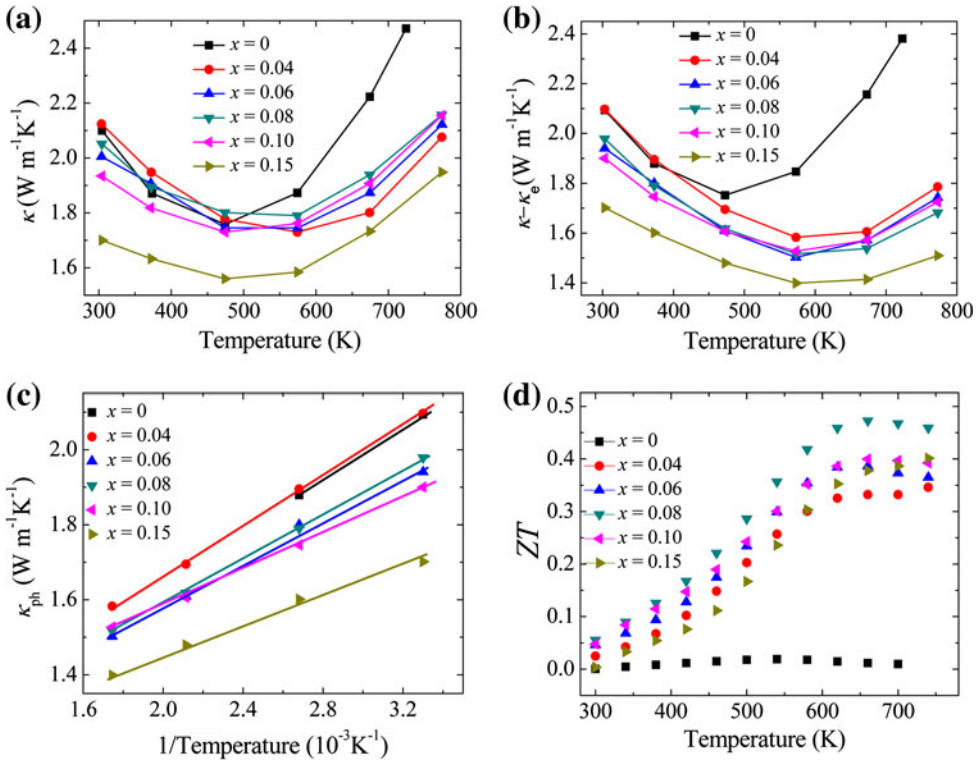

Fig. 3. Temperature dependences of (a) thermal conductivity κ, (b) $\kappa - \kappa_e$, (c) $\kappa_{ph} \propto 1/T$ relationships at low temperatures and (d) ZT for the $Mg_2Si_{0.5}Sn_{0.5}$-xGaSb ($0 \le x \le 0.15$) samples.

10^{-8} V^2 K^{-2} is used for estimation. The calculated result is plotted in Fig. 3b. The lattice thermal conductivity decreases with increasing GaSb content. The sample with $x = 0.15$ has the lowest lattice thermal conductivity, being about 20% lower than that of the matrix at room temperature. The lattice thermal conductivity of all the samples followed a $1/T$ behavior in the low-temperature region between 300 K and 570 K due to the Umklapp process (Fig. 3c). This is in good agreement with the results for Sb-doped $Mg_2Si_{0.5}Sn_{0.5}$ solid solutions.[18] It is noteworthy that the slope decreases with increasing GaSb content (Fig. 3c). This is due to the decrease of Debye frequency or/and sound velocity according to the relationship $\kappa_{ph} \propto Rh v_s \omega_D / 2\pi k_B T$,[20] where R, h, v_s, ω_D, and k_B are the gas constant, Planck constant, sound velocity, Debye frequency, and Boltzmann constant, respectively.

Based on the measured electrical and thermal properties, the temperature dependence of the dimensionless figure of merit was calculated and is shown in Fig. 3d. A maximum dimensionless figure of merit of 0.47 at 660 K was obtained at $x = 0.08$. It should be noted that all the samples show semiconducting behavior due to low carrier concentration. High-performance TE materials are usually heavily doped semiconductors. Given further optimization of electrical transport properties via Sb or Bi doping, $Mg_2Si_{0.5}Sn_{0.5}$-xGaSb TE materials are expected to achieve higher ZT values.

CONCLUSIONS

Single-phase $Mg_2Si_{0.5}Sn_{0.5}$-xGaSb ($0 \le x \le 0.15$) solid solutions were prepared by B_2O_3 flux method followed by hot pressing. The Seebeck coefficient in the high temperature range and the electrical conductivity of samples with added GaSb were enhanced as compared with the matrix. The lattice thermal conductivity shows a T^{-1} dependence, indicative of the Umklapp process, and decreases monotonically with increasing GaSb amount. The composition with the highest GaSb content results in a reduction in room-temperature lattice thermal conductivity of 20% as compared with that of $Mg_2Si_{0.5}Sn_{0.5}$. As a result, a maximum ZT of 0.47 was obtained at 660 K for $x = 0.08$, obviously higher than that of the matrix.

ACKNOWLEDGEMENTS

The work was supported by the National Natural Science Foundation of China (50731006, 50971115, and 51061120455) and the Natural Science Foundation of Zhejiang Province (Z4090204).

REFERENCES

1. T.M. Tritt, *Science* 272, 1276 (1996).
2. F.G. Disalvo, *Science* 285, 703 (1999).
3. J.J. Shen, T.J. Zhu, X.B. Zhao, S.N. Zhang, S.H. Yang, and Z.Z. Yin, *Energy Environ. Sci.* 3, 1519 (2010).
4. J.P. Heremans, V. Jovovic, E.S. Toberer, A. Saramat, K. Kurosaki, A. Charoenphakdee, S. Yamanaka, and G.J. Snyder, *Science* 321, 554 (2008).

5. V.K. Zaitsev, M.I. Fedorov, E.A. Gurieva, I.S. Eremin, P.P. Konstantinov, A.Y. Samunin, and M.V. Vedernikov, *Phys. Rev. B* 74, 045207 (2006).
6. Q. Zhang, J. He, T.J. Zhu, S.N. Zhang, X.B. Zhao, and T.M. Tritt, *Appl. Phys. Lett.* 93, 102109 (2008).
7. X.H. Ji, J. He, Z. Su, N. Gothard, and T.M. Tritt, *J. Appl. Phys.* 104, 034907 (2008).
8. S.N. Zhang, T.J. Zhu, S.H. Yang, C. Yu, and X.B. Zhao, *Acta Mater.* 58, 4160 (2010).
9. S.R. Brown, S.M. Kauzlarich, F. Gascoin, and G.J. Snyder, *Chem. Mater.* 18, 1873 (2006).
10. K.F. Hsu, S. Loo, F. Guo, W. Chen, J.S. Dyck, C. Uher, T. Hogan, E.K. Polychroniadis, and M.G. Kanatzidis, *Science* 303, 818 (2004).
11. S.H. Yang, T.J. Zhu, T. Sun, S.N. Zhang, X.B. Zhao, and J. He, *Nanotechnology* 19, 245707 (2008).
12. J. Tani and H. Kido, *Intermetallics* 16, 418 (2008).
13. J. Tani and H. Kido, *J. Alloys Compd.* 466, 335 (2008).
14. M.I. Fedorov, V.K. Zaitsev, I.S. Eremin, E.A. Gurieva, A.T. Burkov, P.P. Konstantinov, M.V. Vedernikov, A.Yu. Samunin, G.N. Isachenko, and A.A. Shabaldin, *Phys. Solid State* 48, 1486 (2006).
15. G.S. Nolas, D. Wang, and M. Beekman, *Phys. Rev. B* 76, 235204 (2007).
16. M. Riffel and J. Schilz. *Proc. 15th Int. Conf. on Thermoelectrics*, 1996, p. 133.
17. Q. Zhang, J. He, X.B. Zhao, S.N. Zhang, T.J. Zhu, H. Yin, and T.M. Tritt, *J. Phys. D Appl. Phys.* 41, 185103 (2008).
18. H.L. Gao, T.J. Zhu, X.X. Liu, L.X. Chen, and X.B. Zhao, *J. Mater. Chem.* 21, 5933 (2011).
19. A. Kato, T. Yagi, and N. Fukusako, *J. Phys. Condens. Matter* 21, 205801 (2009).
20. S. Kasap, *Principles of Electrical Engineering Materials and Devices*, 2nd ed. (New York: McGraw Hill, 1997).